

https://doi.org/10.1070/QEL16456

Formation of carbon quantum dots and nanodiamonds in laser ablation of a carbon film

A.I. Sidorov, V.F. Lebedev, A.A. Kobranova, A.V. Nashchekin

Abstract. **We have experimentally shown that nanosecond near-IR pulsed laser ablation of a thin amorphous carbon film produces carbon quantum dots with a graphite structure and nanodiamonds with a characteristic size of 20–500 nm on the substrate surface. The formation of these nanostructures is confirmed by electron microscopic images, luminescence spectra and Raman spectra. The mechanisms explaining the observed effects are proposed.**

Keywords: *carbon film, carbon quantum dot, nanodiamond, laser ablation.*

1. Introduction

Laser evaporation and laser ablation methods are widely used for nanostructuring surfaces and forming nanoparticles of various materials [1–3]. These methods allow dielectric [4], semiconductor [5] and metal nanoparticles [6–8] to be formed on a surface. Laser evaporation and ablation of a target with deposition of nanoparticles on a substrate have, in comparison with other methods, a number of advantages, primarily due to their simplicity and high productivity. Laser ablation makes it possible to obtain not only nanoparticles whose structure and composition reproduce the structure and composition of the target, but also to produce nanoparticles with completely different structural and chemical characteristics (see, for example, [7–9]).

Carbon quantum dots (CQDs) and nanodiamonds (NDs) have unique properties and may potentially be used in chemical and biological sensors [10, 11], in dosimeters [12, 13], in electro- and photocatalysis [14, 15], in biological object imaging [16, 17] and in optoelectronics and photovoltaics [18–21]. CQDs and NDs intensively luminesce in the blue and red spectral regions, respectively [22, 23]. With the use of doping, it is possible to shift their luminescence bands over a wide range along the spectrum. In addition, NDs are promising for the formation of metamaterials [24].

For the CQD synthesis, the pyrolysis method of organic compounds is widely used [25], and NDs are synthesised by the detonation method [26], by plasma deposition from vapours of organic compounds [27–29] and by magnetron sputtering [30]. Recently, a method of femtosecond laser ablation of organic liquids has become widely used for the ND synthesis [2, 9]. At the same time, local synthesis of CQDs and NDs on the substrate surface using the solid-phase method is of practical interest, which will make it possible to use CQDs and NDs in micro- and nanoelectronics as micro- and nanosized light sources, and also in microsensors, for example in microfluidic sensory devices [31].

The purpose of this work is to investigate the possibility of synthesising CQDs and NDs by nanosecond near-IR pulsed laser ablation of an amorphous carbon film.

2. Experimental

In our experiments we used 30-nm-thick films of amorphous carbon, obtained by vacuum deposition on a cold substrate of silicate glass. Ablation was performed using single pulses of the first harmonic (λ = 1064 nm) of an LQ-129 multimode Nd:YAG laser (Solar). The laser pulse duration was 38 ns. The average laser pulse energy density E was chosen in such a way that only the carbon film was subjected to ablation without damaging the substrate (glass) and constituted 18.4 J cm^{-2}. The laser beam diameter on the substrate surface was 0.7 mm. As was shown in [8], nanosecond laser ablation most effectively separates nanoparticles from a torch on the substrate surface if the surface on which the ablation occurs is covered by glass or a transparent material. This spatially constraints the plasma expansion from the laser torch and also limits the region in which the shock wave moves. Therefore, under laser irradiation, the carbon film surface was covered with a polished plate of silicate glass.

Electron microscopic images of the irradiated film zones were obtained with a JEOL JSM 7001F scanning electron microscope (SEM). An additional coating ensuring the charge drain was not applied to avoid loss of information from nanoscale particles. To measure the luminescence spectra in irradiated zones, a LOMO MCFU-K luminescence microscope was used. Raman spectra were measured using an inVia Raman microscope spectrometer (Renishaw). Spectral measurements were performed at room temperature.

3. Experimental results and their discussion

Figure 1a shows a photograph of the irradiated zone of the carbon film. It is seen that the region of the laser action consists of three concentric sections: central part 1 which was directly ablated, black ring 2 which appeared along the laser torch perimeter, and also light coloured region 3 formed by expanding the recombination plasma and the accompanying

A.I. Sidorov, V.F. Lebedev, A.A. Kobranova ITMO University, Kronverskii prosp. 49, 197101 St. Petersburg, Russia;
e-mail: aisidorov@oi.ifmo.ru;
A.V. Nashchekin Ioffe Institute, Russian Academy of Sciences, Polytekhnicheskaya ul. 26, 194021 St. Petersburg, Russia,
e-mail: nashchekin@mail.ioffe.ru

Received 24 June 2017
Kvantovaya Elektronika **48** (1) 45–48 (2018)
Translated by M.A. Monastyrskiy

shock wave. Figure 1b presents a luminescence photograph of the irradiated zone of the carbon film. It can be seen that blue luminescence appeared in regions 1 and 3, while red luminescence – in region 2. In region 2, some inclusions with white luminescence are also visible. At a lower pulse energy density, or when a glass plate is removed from the substrate surface, only blue luminescence appears, mainly in region 3 (see the inset in Fig. 1b).

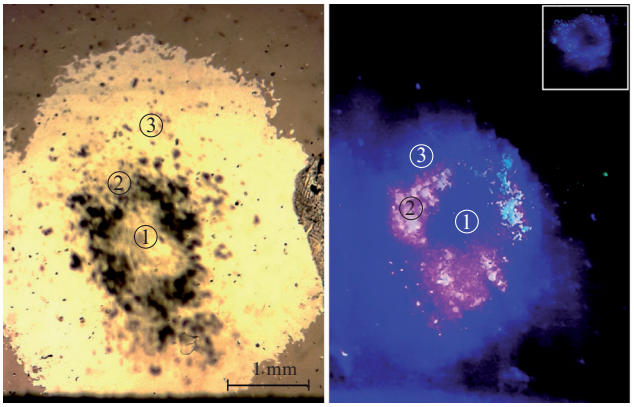

Figure 1. (Colour online) Photographs of (a) the irradiated zone of the carbon film and (b) luminescence of this zone. The inset shows the result of ablation in the absence of an additional glass plate. The luminescence excitation wavelength is 405 nm.

The presence of luminescence indicates the appearance of structural changes in the initially amorphous carbon film during laser ablation. Two-colour luminescence allows us to conclude that at least two types of carbon structures appear in the irradiated zone. Figure 2 shows SEM images of regions 2 and 3 (see Fig. 1a) of the carbon film after laser ablation. It is seen that in region 3 nanoparticles were formed as elongated ellipsoids (Fig. 2a), with the long axes of the ellipsoids oriented along the direction of the shock wave propagation. The characteristic size of the ellipsoids is 20–300 nm. In region 2, nanoparticles appeared in the form of randomly oriented irregular parallelepipeds and cubes (Fig. 2b). Their characteristic size varies from 30 to 500 nm. In this region, nanoparticles of less than 100 nm in size are also present, having a shape close to spherical.

The luminescence spectra of regions 2 and 3 are shown in Fig. 3. The luminescence band of region 3 has a maximum at $\lambda = 460$ nm [curve (*1*)]. The band width constitutes ~130 nm. This luminescence is typical of CQDs [21, 22, 25, 32]. A similar spectrum is observed in the luminescence of region 1 (see Fig. 1b). The luminescence spectrum of region 2 consists of two bands [curve (*2*)]. The short-wavelength band has a maximum at $\lambda = 460$ nm, which indicates the presence of a CQD in region 2. The maximum of the long-wavelength luminescence band corresponds to $\lambda = 570$ nm, while its width is 150 nm. This luminescence is typical of NDs [33]. The appearance of white luminescence in some areas of region 2 (see Fig. 1b) may be stipulated by the increased concentration of CQDs in these areas. This leads to an increase in the blue luminescence intensity in these regions and to the appearance of broadband glowing in the entire visible region of the spectrum.

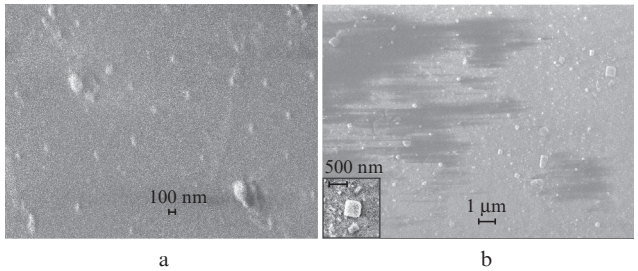

Figure 2. SEM images of regions (a) 3 and (b) 2 in Fig. 1a.

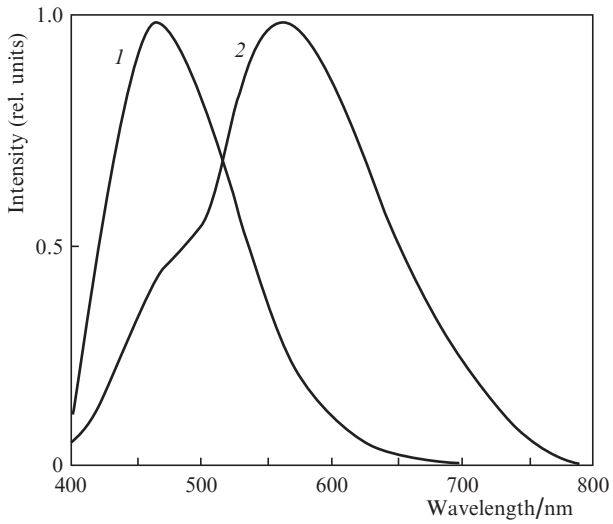

Figure 3. Normalised luminescence spectra of regions (*1*) 3 and (*2*) 2 in Fig. 1a. The excitation wavelength is 400 nm.

Additional information about the results of laser ablation of an amorphous carbon film is given by the Raman spectra shown in Figs 4 and 5. Two pronounced bands with maxima at frequencies of 1360 and 1550 cm^{-1} are observed in the spectrum for region 3 (Fig. 4) and also a weakly pronounced band with a maximum at a frequency of 2100 cm^{-1}. The first two bands (usually denoted as D and G, respectively) are associated with sp^3- and sp^2-hybridisation of carbon, characteristic of the crystalline structure of graphite [34]. The broadening of the bands is caused by a partial disordering of the crystal CQD structure. A weakly pronounced band (maximum at a frequency of 2100 cm^{-1}) may be due to the presence of carbon in the form of carbyne (molecular chains of carbon) in region 3. The appearance of this band may be caused by oscillations in the form of stretching of C – C bonds (R-mode) [35, 36].

The Raman spectrum of region 2 has a more complicated form (Fig. 5) and represents a superposition of several bands. This indicates the presence of carbon in several states in the given region, which is also confirmed by the SEM image of region 2 shown in Fig. 2b. A narrow band at a frequency of 1310 cm^{-1} corresponds to the D-mode of NDs [36, 37]. A wide band with a maximum at a frequency of 1360 cm^{-1} can be associated with the B-mode of CQDs. A band with a maximum at a frequency of 1600 cm^{-1} is associated with the presence of amorphous carbon (G-mode) in region 2 [38].

Thus, nanosecond laser ablation of an amorphous carbon film leads to structural changes both within the ablation

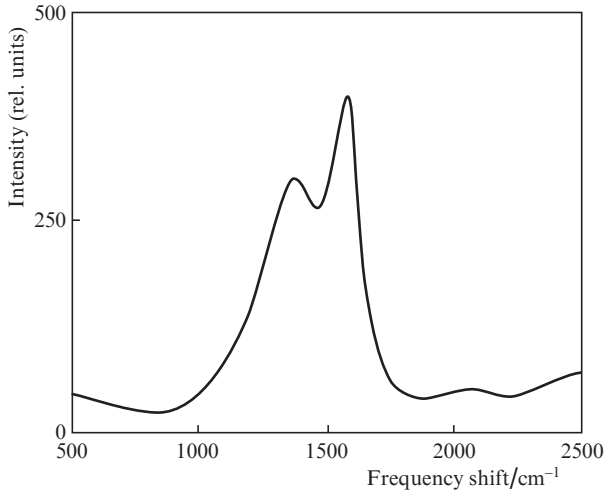

Figure 4. Raman scattering spectrum of region 3 in Fig. 1a.

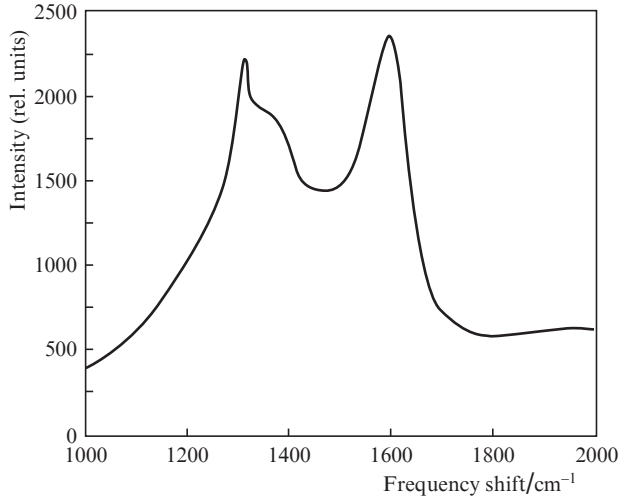

Figure 5. Raman scattering spectrum of region 2 in Fig. 1a.

region and at its periphery. Directly in the region of the laser beam action, CQDs are formed on the substrate surface. CQDs, carbines and NDs arise along the laser torch perimeter. The latter have the form of cubes or parallelepipeds with a characteristic size of 30–500 nm. Carbines and CQDs of ellipsoidal shape with a characteristic size of 20–300 nm appear in the recombination plasma expansion region. The formation of nanoparticles with chemical and structural properties being different from film or substrate was observed, in particular, in [7, 8]. In these works, in laser ablation (using a Nd:YAG laser) and laser evaporation (using a CO_2 laser) of silicate glasses containing silver ions, a thin layer of silver nanoparticles was formed inside the ablation zone on the glass surface. A ring with a high concentration of silver nanoparticles of ellipsoidal shape appeared on the glass surface in the region of recombination plasma along the laser torch perimeter. It was shown in [7, 8] that nanoparticles are formed immediately after the laser action when plasma is cooled, and recombination and chemical processes take place in it. Thus, the plasma chemical components take the structural forms, which are the most energetically favourable for the given substance under the given conditions. In the ablation region, CQDs arise after the laser pulse termination, at the stage of cooling the dense plasma at a relatively low temperature. NDs are formed at the laser pulse final stage, when the temperature in the recombination plasma region is still high, and a shock wave is formed, creating a high pressure in this region. The presence of an additional glass plate on the carbon film leads to an increase in the shock wave pressure and ND formation efficiency. The conditions for the ND formation in this case are close to those that are realised in the ND synthesis by the detonation method [26]. In the expansion region of recombination plasma, CQDs arise after the laser pulse termination at sufficiently 'soft' temperature conditions and not very high pressures. At a low pulse energy density or in the absence of an additional glass plate, the conditions realised during laser ablation do not ensure the ND formation; therefore, in all three regions, mainly CQDs are formed.

4. Conclusions

The experimental results presented in this paper show that, in laser ablation of an amorphous carbon film by nanosecond laser pulses, CQDs with a graphite structure and NDs can be formed on the substrate surface in the ablation zone and around it. The characteristic sizes of CQDs and NDs are 20–300 nm and 30–500 nm, rspectively. Nanodiamonds are formed mainly around the laser torch perimeter at the boundary of the recombination plasma region, while CQDs are formed both directly in the ablation region and around it in the expansion region of the recombination plasma. Since CQDs and NDs can be locally formed in a small area, the results obtained can be used to design microscale chemical and biological sensors, as well as microfluidic devices.

Acknowledgements. This work was supported by the Ministry of Education and Science of the Russian Federation (Project No. 16.1651.2017 / 4.6). SEM images were obtained using the equipment of the Federal Shared Facilities Centre 'Materials Science and Diagnostics in Advanced Technologies', supported by the Ministry of Education and Science of the Russian Federation (Project Unique Identifier RFMEFI62117X0018).

References

1. Bäuerle D. *Laser Processing and Chemistry* (Berlin–Heidelberg: Springer-Verlag, 2011).
2. Yang G.W. *Progr. Mater. Sci.*, **52**, 648 (2007).
3. Zavestovskaya I.N. *Quantum Electron.*, **40**, 942 (2010) [*Kvantovaya Elektron.*, **40**, 942 (2010)].
4. Osipov V.V., Platonov V.V., Lisenkov V.V. *Quantum Electron.*, **39**, 541 (2009) [*Kvantovaya Elektron.*, **39**, 541 (2009)].
5. Bulgakov A.V., Evtushenko A.B., Shukhov Yu.G., Ozerov I., Marin V. *Quantum Electron.*, **40**, 1021 (2010) [*Kvantovaya Elektron.*, **40**, 1021 (2010)].
6. Amoruso S., Ausanio G., Bruzzese R., Vitiello M., Wang X. *Phys. Rev. B*, **71**, 033406 (2005).
7. Egorov V.I., Nashchekin A.V., Sidorov A.I. *Quantum Electron.*, **45**, 858 (2015) [*Kvantovaya Elektron.*, **45**, 858 (2015)].
8. Egorov V.I., Zvyagin I.V., Klyukin D.A., Sidorov A.I. *Opt. Zh.*, **81** (5), 54 (2014).
9. Nee C.-H., Yap S.-L., Tou T.-Y., Chang H.-C., Yap S.-S. *Sci. Reports*, **6**, 33966 (2016).
10. Zhao H.X., Liu L.Q., Liu Z.D., Wang Y., Zhao X.J., Huang C.Z. *Chem. Commun.*, **47**, 2604 (2011).
11. Zhou L., Lin Y., Huang Z., Ren J., Qu X. *Chem. Commun.*, **48**, 1147 (2012).

12. Ade N., Nam T.L., Derry T.E., Mhlanga S.H. *Radiat. Phys. Chem*., **98**, 155 (2014).
13. Gorka B., Nilsson B., Svensson R., Brahme A., Ascarelli P., Trucchi D.M., Conte G., Kalish R. *Phys. Med.*, **24**, 159 (2008).
14. Hu C., Yu C., Li M., Wang X., Dong Q., Wang G. *Chem. Commun*., **51**, 3419 (2015).
15. Li H., Sun C., Ali M., Zhou F., Zhang X., MacFarlane D.R. *Angew. Chem. Int. Ed.*, **54**, 8420 (2015).
16. Jiang K., Sun S., Zhang L., Wang Y., Cai C., Lin H. *ACS Appl. Mater. Interfaces*, **7**, 23231 (2015).
17. Chizhik A.M., Stein S., Dekaliuk M.O., Battle C., Li W., Huss A. *Nano Lett*., **16**, 237 (2016).
18. Zhang C.M., Lin J. *Chem. Soc. Rev*., **41**, 7938 (2012).
19. Lim S.Y., Shen W., Gao Z.Q. *Chem. Soc. Rev.*, **44**, 362 (2015).
20. Ortega-Liebana M.C., Hueso J.L., Larrea A., Sebastian V., Santamaria J. *Chem. Commun*., **51**, 16625 (2015).
21. Ortega-Liebana M.C., Hueso J.L., Ferdousi S., Yeung K.L., Santamaria J. *Diamond Relat. Mater*., **65**, 176 (2016).
22. Nelson D.K., Razbirin B.S., Starukhin A.N., Eurov D.A., Kurdyukov D.A., Stovpiaga E.Y., Golubev V.G. *Opt. Mater*., **59**, 28 (2016).
23. Stehlik S., Ondic L., Berhane A.M., Aharanivic I., Girard H.A., Arnault J., Rezek B. *Diamond Relat. Mater*., **62**, 91 (2016).
24. Shalaginov M.Y., Naik G.V., Ishii S., Slipchenko M.N., Boltasseva A., Cheng J.X., Smolyaninov A.N., Kochman E., Shalaev V.M. *Appl. Phys. B*, **105**, 191 (2011).
25. Zhu S., Meng Q., Wang L., Zhang J., Song Y., Jin H. *Angew. Chem. Int. Ed*., **52**, 3953 (2013).
26. Danilenko V.V. *Phys. Solid State*, **46**, 595 (2004).
27. Angus J.C. *Diamond Relat. Mater*., **49**, 77 (2014).
28. Gracio J.J., Fan Q.H., Madaleno J.C. *J. Phys. D: Appl. Phys.*, **43**, 374017 (2010).
29. Sankaran R.M., Giapis K.P. *J. Appl. Phys*., **92**, 2406 (2002).
30. Wu Z., Tian X., Gui G., Gong C., Yang S., Chu P.K. *Appl. Surf. Sci*., **276**, 31 (2013).
31. Zhang D., Men L., Chen Q. *Sensors*, **2**, 5360 (2011).
32. Li Y., Zhong X., Rider A.E., Furmand S.A., Ostrikov K. *Green Chem*., **16**, 2566 (2014).
33. Khomich A.A., Kudryavtsev O.S., Dolenko T.A., Shiryaev A.A., Fisenko A.V., Konov V.I., Vlasov I.I. *Laser Phys. Lett*., **14**, 025702 (2017).
34. Esmeryan K.D., Castano C.E., Bressler A.H., Abolghasemibizaki M., Fergusson C.P., Roberts A., Mohammad R. *Diamond Relat. Mater*., **75**, 58 (2017).
35. Milani A., Tommasini M., Russo V., Bassi A.L., Lucotti A., Cataldo F., Beilstein J. *Nanotechnol*., **6**, 480 (2015).
36. Buntov E.A., Zatsepin A.F., Guseva M.B., Ponosov Y.S. *Carbon*, **117**, 271 (2017).
37. Mochalin V.N., Shenderova O., Ho D., Gogotsi Y. *Nature Nanotechnol*., **7**, 11 (2012).
38. Inzoli F., Dellasega D., Russo V., Caniello R., Conti C., Ghezzi F., Passoni M. *Diamond Relat. Mater*., **74**, 212 (2017).